

Graphene Shape Control by Multistage Cutting and Transfer

By Lijie Ci,* Li Song, Deep Jariwala, Ana Laura Elías, Wei Gao, Mauricio Terrones, and Pulickel M. Ajayan*

The fascinating properties of graphene render it very promising for electronics applications, such as field-effect transistors and interconnects. For these applications, appropriate processes are required to tailor graphene sheets into desired geometries with specific dimensions, smooth edges, and specific edge types.^[1–5] By combining electron-beam lithography and plasma etching,^[6,7] graphene nanoribbon devices have been fabricated and tested. However, the production of graphene devices with smooth edges, well-defined shapes, and controlled edge configuration (zigzag or armchair edged) is still a challenge. Nanocutting of graphene sheets has been realized using nanometer-sized nickel^[8] or iron particles^[9] in hydrogen atmosphere at high temperatures, a process referred to as catalytic hydrogenation.^[10–13] This nanocutting process can generate various shapes of graphene pieces. The edges of these pieces are along specific crystallographic orientations, which can be controlled by the size of the catalyst particles.^[8] Theoretically and experimentally, we have shown that the edges of cutting channels can be atomically smooth with zigzag or armchair terminations. It is well known that scattering of electrons, the charge carriers, at a rough graphene edge will decrease their mean free path.^[7,14] Therefore, the catalytic cutting technique provides an efficient approach to fabricating graphene components with high electron conductivity. Another important finding in our previous work is that catalyst particles bounce back at angles of 60° or 120° when they approach a free edge,^[8] which means that cutting always proceeds along the same crystallographic orientation. With the change in

orientation occurring at 60° or 120°, it is possible to cut graphene pieces into various shapes with the same edge type, for example in triangles, and this could impact applications such as shape-enhanced magnetism in graphene materials.^[15,16]

Here we report a novel multistage cutting technique for graphene that is able to produce specific well-defined shapes that could be useful in the fabrication of graphene devices. In our study, scanning electron microscopy (SEM) observations (FEI Company, Quanta 400 ESEM FEG) indicate that most of the cut channels start from step edges of graphene (Fig. 1a). This is due to

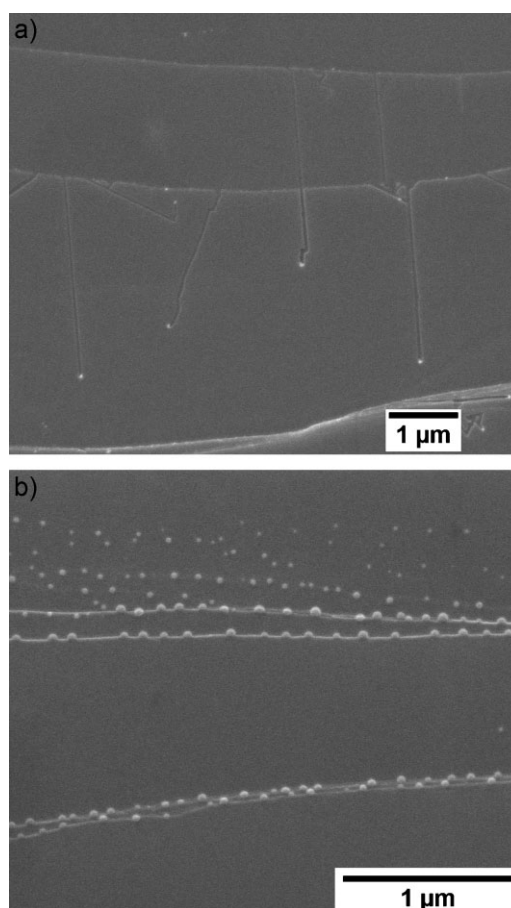


Figure 1. Graphene nanocutting always starts from step edges, as catalyst nanoparticles tend to form at the step edges. a) SEM image showing nanocutting starting from several step edges on HOPG. b) SEM image of nanoparticles formed along step edges after high-temperature annealing.

[*] Dr. L. Ci, Prof. P. M. Ajayan, Dr. L. Song
Department of Mechanical Engineering and Materials Science
Rice University
Houston, TX 77005 (USA)
E-mail: levici2002@yahoo.com; ajayan@rice.edu

D. Jariwala
Department of Metallurgical Engineering
Institute of Technology, Banaras Hindu University (IT-BHU)
Varanasi 221005 (India)

Dr. A. L. Elías, Prof. M. Terrones
Advanced Materials Department
Institute for Scientific and Technological Research of San Luis Potosí (IPICyT)
Camino Presa San José 2055
78216, San Luis Potosí, S.L.P. (Mexico)

W. Gao
Department of Chemistry
Rice University
Houston, TX 77005 (USA)

DOI: 10.1002/adma.200900942

metal nanoparticles tending to nucleate and grow at step edges.^[17,18] In a control experiment using only Ar gas flow (other conditions were the same), we showed that there were no cutting channels, most of the catalyst particles were distributed along step edges (Fig. 1b), and there were almost no particles on terraces. Step edges on graphene can be manually created by a couple of methods, such as oxidation gasification reaction,^[19] ion beam bombardment,^[18] and plasma etching.^[20] The etched step edges can act as nucleation centers for metal catalyst particles, so that the position of the initial cutting site is defined. Based on this assumption, we successfully designed and performed experiments to obtain cut graphene pieces suitable for electronic device fabrication.

Our first experimental design is based on the multistage cutting process. This process can increase the density of cut regions. Small pits were initially etched by an oxidation gasification process^[19] on the surface of highly ordered pyrolytic graphite (HOPG), and these pits, along with the original step edges, act as nucleation centers for catalyst particles during the first cutting process. Note that pits can be patterned on HOPG,^[18] so that better controlled cutting based on patterned etch pits is possible. For the multistep cutting process, following the first cutting, we deposited catalyst particles for a second time, and once again the new channel edges act as nucleation centers for nanoparticle formation during this second cutting step. This process can be repeated several times. Figure 2 shows typical results of a multistage cutting process. The oxidation etching process was carried out at 650 °C in air, and the etching time lasted for 1–5 min. After etching, nearly hexagonal pits are observed on the surface of the HOPG (Fig. 2a). Catalyst deposition was then performed by a dip-coating process.^[8]

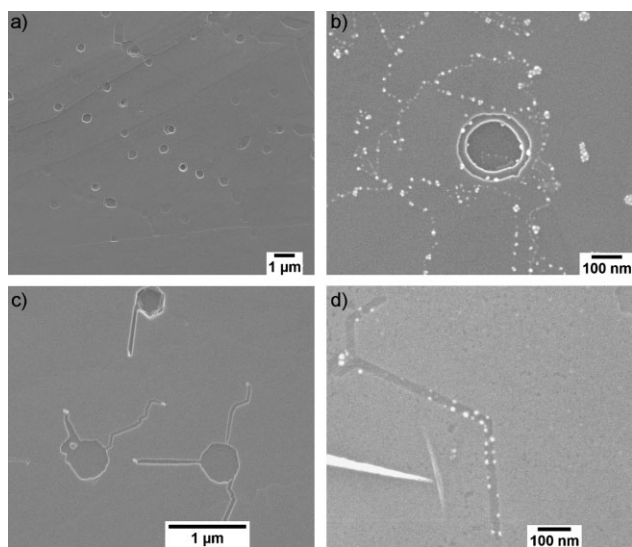


Figure 2. Manually created edges can be nucleation centers for catalyst particles for high-density graphene cutting. a) SEM image of etch pits formed on the HOPG surface after 5 min oxidative etching at 650 °C in air. b) SEM image of catalyst nanoparticles formed along the edges of etch pits and original step edges after 500 °C annealing. c) SEM image of short nanocut channels starting from etch pits during the first cutting step. d) SEM image showing that nanoparticles also form along the edge of cut channels after the second catalyst deposition step.

Figure 2b shows the distribution of catalyst particles after annealing for 1 h at 500 °C. Most of the catalyst particles are located either at the edges of pits or at other step edges. During the first cutting step, channels are created starting from pit edges and original step edges. Figure 2c shows some of the short channels that originated from the edges of pits. We noticed that most of the channels formed during the first cutting are very short. Our results indicate that the surface of HOPG becomes inert to cutting after a long period of oxidation etching (>10 min). Figure 2d shows that metal nanoparticles are also formed along the cut edges of channels (bright dots) after the annealing process following the second catalyst deposition. After the second cutting

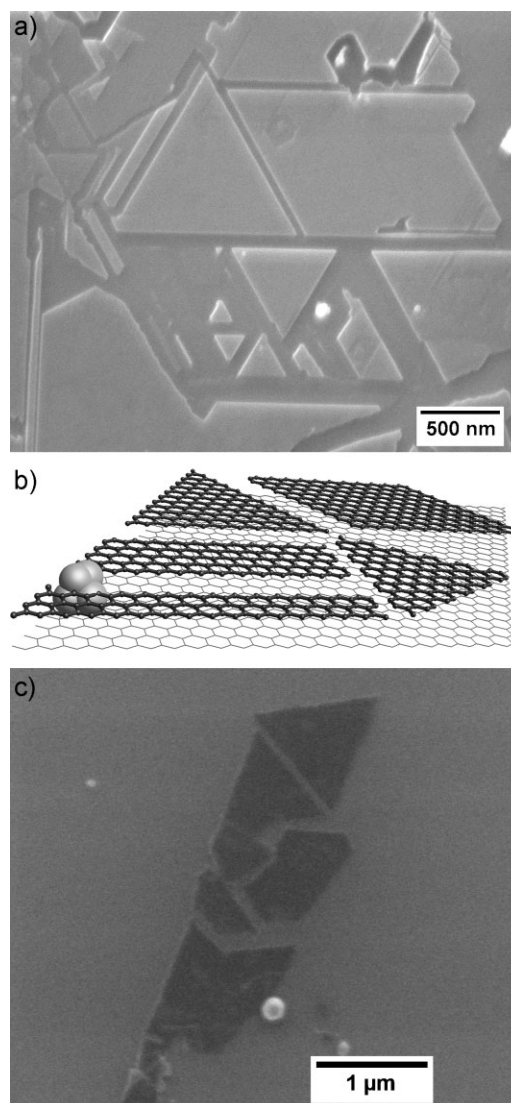


Figure 3. A multistage cutting process can produce a high density of separate cut pieces on a HOPG surface for easy transfer. a) SEM image showing the very dense organization of graphene cut pieces on the surface of HOPG after the second step of cutting. b) Molecular model of differently shaped graphene pieces obtained by multistage cutting: the cut pieces can have either armchair or zigzag edges. c) SEM image of several cut graphene pieces that have been transferred onto the surface of a Si wafer.

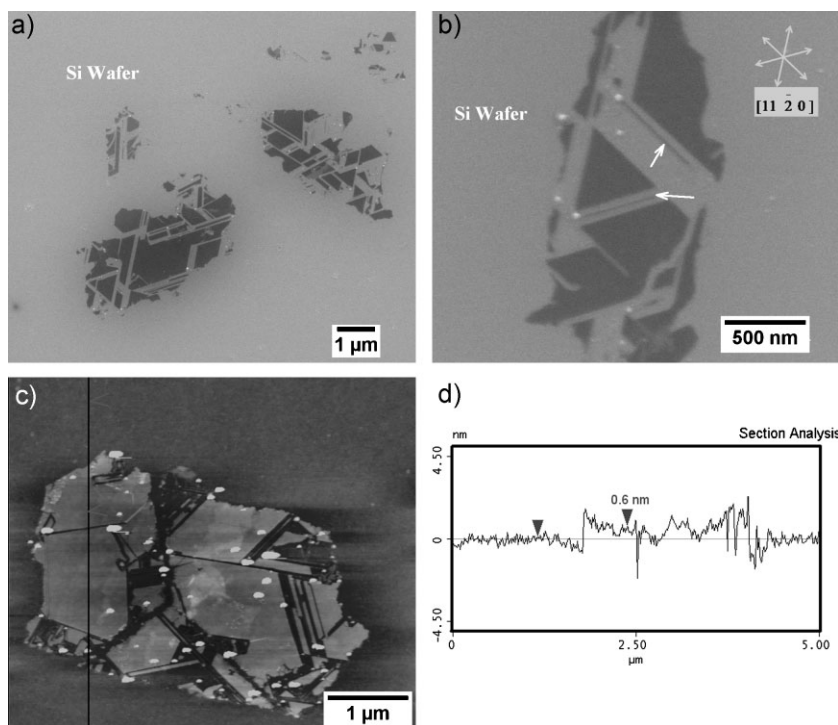


Figure 4. Nanocutting of graphene fragments transferred onto Si surfaces. a) SEM image showing that all the graphene fragments have been cut into small pieces. b) Most of the cut channels are along the same directions in single graphene fragments. SEM showing the edges of a triangle shape and two nanoribbons formed along the $[11\bar{2}0]$ orientation. c,d) AFM image and thickness analysis showing that a single-layer graphene fragment was cut into small pieces of various shapes. Owing to an epoxy nanogluue layer remaining under the piece, some of the portions show thicker profiles.

step, as Figure 3a shows, the top surface of HOPG is fully patterned with well-defined shapes of cut graphene layers. Some of the pieces are perfect equilateral triangles, and some are rectangles or ribbons of different sizes. Cutting during the second step seems to be more efficient than during the first cutting process, since the etched areas on the top HOPG surface increase with each cutting step. The edges of the cutting pieces could be either zigzag or armchair terminated, as the molecular model shows (Fig. 3b).

The isolated cut pieces of graphene on the top surface of HOPG could be transferred to other substrates for any practical uses, and this can be easily accomplished. Figure 3c shows transferred graphene pieces on a Si wafer using an ultrathin epoxy film as an adhesive layer (for details please see the Supporting Information). However, this transfer method is limited by the lack of uniformity and flatness of the surface of large HOPG blocks used in the experiment. A more effective transfer technique is being developed. For example, the recently reported electrostatic-force-assisted method could be used to transfer our graphene cut pieces,^[21] and we are in the process of optimizing this method. For device applications, it is desirable to have the cut graphene pieces on the surface of a Si wafer. For this purpose, we have developed an alternative technique, in which large graphene fragments are first transferred onto a Si wafer; the edges of these fragments can act as catalyst nucleation centers,

similar to the oxidation pits described earlier. This avoids the oxidation process used for the creation of pits leading to defects in the top graphene layers, hence affecting the charge transport of the devices.^[22]

One approach to placing graphene fragments on a Si wafer is the micromechanical cleavage method.^[2] However, this procedure is complex and the yield of thin graphene pieces is very low. Therefore, we have developed a highly efficient and productive method to directly transfer thin graphene fragments onto a Si wafer in large quantities (for more details, see Supporting Information). Briefly, we used an ultrathin epoxy film as an adhesive layer to bond large graphite fragments on a Si wafer. Graphite fragments can be repeatedly peeled (with sticky tape or ultrasonication) until they become thin enough to be useful. Extra epoxy coating on Si can be removed by an etching process at 500 °C in air. Once the graphene fragments were transferred onto Si, catalyst particles were deposited using the usual dip-coating process. Cutting was performed at temperatures ranging from 800 °C to 1000 °C. However, we found that cutting at 850 °C yields the best result for cutting on a Si wafer (see Fig. 4a). Cutting channels at this temperature are very straight, which ultimately results in very regular triangles, rectangles, and ribbon shapes.

One of the important features in our observations is that most of the transferred graphene fragments are single-crystalline domains. We find that cutting in any graphene fragments occurs mainly along the same crystallographic orientation. As Figure 4b shows, these cuts are believed to occur along the $[11\bar{2}0]$ direction, as analyzed in our previous report.^[8] Our atomic force microscopy (AFM, Digital Instruments Nanoscope IIIA) investigation indicates that most channels are etched down to the Si surface, which means the cut pieces are isolated from one another. Catalyst particles move back and forth either straight or at 60° or 120° between the edges and the cutting channels, and cut the large graphene fragments into smaller pieces having ribbon-shaped and triangular geometries. Figure 4b shows that an equilateral triangle-shaped graphene piece and two graphene nanoribbons (indicated by white arrows) are formed. Based on our previous results, all these graphene pieces could be zigzag edged.^[8] Theoretical modeling indicates that graphene pieces with zigzag edges have specific magnetic properties, and they can be used in future spintronics applications.^[15,16] We performed AFM section analysis to determine the thickness of the cut graphene pieces on the Si surface. It is easy to find single-layer or few-layer graphene pieces, as shown in Figure 4c and d.

The above two procedures (multistage cutting and transfer onto Si and cutting) indicate that it is very efficient to promote the nanocutting by creating more step edges in a large graphene surface. For real applications, it is desirable to be able to control the locations of the edges, so that cutting positions can be

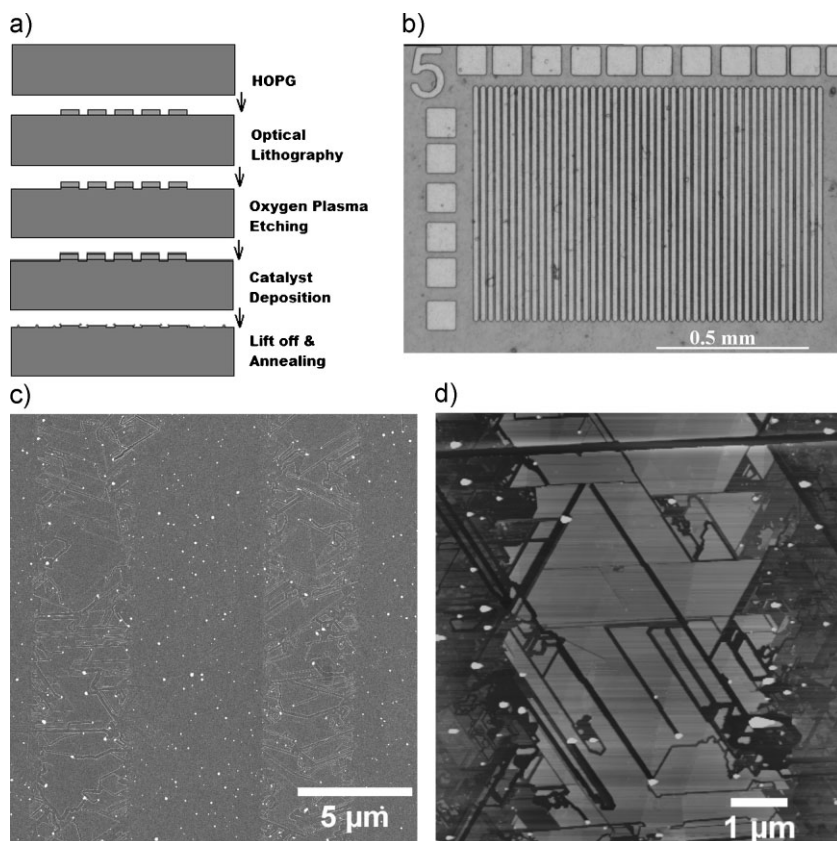


Figure 5. Position control of graphene nanocutting can be achieved by a patterned cutting process. a) Process flow for the patterned cutting approach. b) Optical image of ribbon patterns created on a HOPG surface. c) Low-magnification SEM image of cutting channels on a patterned area. Plasma etching time: 1 min. d) AFM image showing that cutting channels on the patterned area form various graphene shapes. Plasma etching time: 30 s.

determined. This can be achieved by combining lithography techniques. We have designed a patterned cutting process. First, a HOPG surface was patterned by lithography, and oxygen plasma was used to etch and form patterned step edges (for more details, please see the Supporting Information). Figure 5a shows the process flow we used for the patterned cutting. First, photoresist was spin-coated a few micrometers thick on the surface of HOPG, and optical lithography was performed in order to form a patterned structure, such as the ribbon patterns shown in the optical image (Fig. 5b). Oxygen plasma etching was then used to etch the exposed graphene layers. After Ni catalyst had been deposited using a thermal evaporator, photoresist was removed in acetone and the cutting process was performed at 850 °C. Figure 5c shows a low-magnification SEM image of the patterned cut graphene after 1 min plasma etching. As expected, on the patterned ribbon (photoresist-covered area), most of the cut channels start from one or other of the edges. Some channels are cut across the whole ribbon (5 μm wide), and some make turns and meet with other channels. The AFM image (Fig. 5d) shows various cut graphene shapes formed on the patterned area. AFM analysis (in the Supporting Information) indicates that the heights of the patterned ribbons reach about 10 nm in 30 s, and about 18 nm in 1 min. The height of the step edges will determine

the thickness of the cut graphene pieces. By controlling the oxygen plasma etching process, thinner patterned edges one or a few graphene layers thick could be created. Because the patterned ribbons are out of the HOPG surface, it should be very easy to transfer all the cut pieces to other substrates for electronics applications.^[21]

In summary, graphene cutting can be promoted by manually creating step edges on large graphene fragments. Combining a lithography technique, graphene transfer method, and multistage cutting, we have come a step closer to being able to create graphene devices with much better edge and shape control. It is worth noting that our approach is efficient, versatile, and could be applied to large-area graphene grown by chemical vapor deposition (CVD)^[23] or transferred by any other technique onto any substrate.

Experimental

Multistage Cutting Process and Transfer: We used a simple oxidation gasification process to create pits or small voids. Freshly peeled HOPG surface was exposed in air at 650 °C for 1–5 min. Pits with diameter up to several hundred nanometers can be created. After oxidative etching, we deposited catalyst by a dip-drawing process. A piece of HOPG was dipped into a 0.2 mmol L⁻¹ NiCl₂/ethanol solution, and then drawn out slowly. After drying in air, the sample was annealed at 500 °C in Ar/H₂ flow (1300 sccm, 15 vol% hydrogen) for 1 h, and then the temperature was immediately increased up to the cutting set point (850–1000 °C). After the first-time cutting, the same catalyst deposition and cutting were repeated.

To transfer graphene nanocut pieces from the HOPG surface to a Si surface, we spin-coated a highly dilute epoxy film on the Si surface. Epoxy/chloroform solution with concentration of 0.02 mg mL⁻¹ was prepared by mixing the resin and hardener in appropriate proportions (7:3) and dissolving the mixture in chloroform. We pressed and clamped the HOPG piece with the cut surface in contact with the epoxy layer. After that, the sample was kept at 140 °C for at least 1 h to cure. After epoxy curing and removal of the HOPG piece, small graphene nanocut pieces can be transferred onto the Si surface.

Transfer and Cutting on Si Wafer: Transferring a high density of large graphene fragments was achieved by first bonding thin graphite pieces to the Si substrate (with 300 nm SiO₂ coating) using epoxy resin and repeatedly peeling them off until they become thin enough to be useful. Various concentrations of epoxy solutions were prepared, ranging from 1.4 × 10⁻⁴ mg mL⁻¹ to 1.7 × 10⁻⁵ mg mL⁻¹. A spin rate of 5000 rpm was used to coat a thin epoxy film on Si. After the Si substrate had been coated with epoxy, small HOPG pieces attached to sticky tape were applied to the Si substrate. The tape was properly pressed against the Si substrate to ensure proper bonding. The piece was then kept at 140 °C in an oven to cure the epoxy. After curing, the tape was peeled off the Si substrate, and the graphite pieces were then repeatedly peeled using fresh sticky tape (about 150 times). After peeling, the Si piece was annealed at 500 °C in air for 30 min to etch away the epoxy and tape glue on Si.

We also used ultrasonication as an alternative to peeling graphite from the Si substrate. After a thick graphite piece had been bonded on the Si, the piece was pretreated at 500 °C for 15 min in air to remove the epoxy. It was

then dipped in acetone and ultrasonicated for varying time intervals. The amount and thickness of the graphene pieces left on were checked under the optical microscope. We found that the best ultrasonication time is 5–10 min.

Patterned Cutting Process: Optical lithography was performed on a freshly peeled piece of HOPG. A spin rate of 3000 rpm was used to coat a photoresist layer on the HOPG surface. The photoresist was exposed under a mask aligner. After developing, the patterned HOPG piece was put into an oxygen plasma chamber (E. A. Fishione Instruments Inc., Model 1020 plasma cleaner, 40W). The etching gas was 25% O₂ with the balance Ar. Etching time ranged from 30 s to 4 min.

Acknowledgements

L.C. and L.S. contributed equally to this work. The authors acknowledge support from the Interconnect Focus Center, one of five research centers funded under the Focus Center Research Program, a Semiconductor Research Corporation program. This work was partially sponsored by CONACYT-Mexico Grants 56787 (Laboratory for Nanoscience and Nanotechnology Research-LINAN) and 58899-Inter American Collaboration (M.T.). The authors are grateful to A. Botello, D. Ramírez, and G. Ramírez for technical assistance. Supporting Information is available online from Wiley InterScience or from the authors.

Received: March 18, 2009

Revised: April 29, 2009

Published online:

[1] M. I. Katsnelson, *Mater. Today* **2007**, *10*, 20.

[2] K. S. Novoselov, A. K. Geim, S. V. Morozov, D. Jiang, Y. Zhang, S. V. Dubonos, I. V. Grigorieva, A. A. Firsov, *Science* **2004**, *306*, 666.

- [3] K. S. Novoselov, A. K. Geim, S. V. Morozov, D. Jiang, M. I. Katsnelson, I. V. Grigorieva, S. V. Dubonos, A. A. Firsov, *Nature* **2005**, *438*, 197.
- [4] Y. Zhang, J. W. Tan, H. L. Stormer, P. Kim, *Nature* **2005**, *438*, 201.
- [5] R. V. Noorden, *Nature* **2006**, *442*, 228.
- [6] F. Schedin, A. K. Geim, S. V. Morozov, E. W. Hill, P. Blake, M. I. Katsnelson, K. S. Novoselov, *Nat. Mater.* **2007**, *6*, 652.
- [7] C. Berger, Z. Song, X. Li, X. Wu, N. Brown, C. Naud, D. Mayou, T. Li, J. Hass, A. N. Marchenkov, E. H. Conrad, P. N. First, W. A. De Heer, *Science* **2006**, *312*, 1191.
- [8] L. Ci, Z. Xu, L. Wang, W. Gao, F. Ding, I. K. Kelly, I. B. Yakobson, P. M. Ajayan, *Nano Res.* **2008**, *1*, 116.
- [9] S. S. Datta, R. D. Strachan, M. S. Khamis, T. A. Charlie Johnson, *Nano Lett.* **2008**, *8*, 1912.
- [10] A. Tomita, Y. Tamai, *J. Phys. Chem.* **1974**, *78*, 2254.
- [11] C. W. Keep, S. Terry, M. Wells, *J. Catal.* **1980**, *66*, 451.
- [12] R. T. K. Baker, R. D. Sherwood, E. G. Derouane, *J. Catal.* **1982**, *75*, 382.
- [13] J. P. Goethel, T. R. Yang, *J. Catal.* **1987**, *108*, 356.
- [14] A. Naeemi, D. J. Meindl, *IEEE Electron Device Lett.* **2007**, *28*, 428.
- [15] W. L. Wang, S. Meng, E. Kaxiras, *Nano Lett.* **2008**, *8*, 241.
- [16] J. Fernández-Rossier, J. J. Palacios, *Phys. Rev. Lett.* **2007**, *99*, 177204.
- [17] C. E. Cross, J. C. Hemminger, R. M. Penner, *Langmuir* **2007**, *23*, 10372.
- [18] Y.-J. Zhu, A. Schnieders, J. D. Alexander, P. T. Beebe, Jr, *Langmuir* **2002**, *18*, 5728.
- [19] H. Chang, A. J. Bard, *J. Am. Chem. Soc.* **1991**, *113*, 5588.
- [20] X. Lu, H. Huang, N. Nemchuk, S. R. Ruoff, *Appl. Phys. Lett.* **1999**, *75*, 193.
- [21] X. G. Liang, S. P. A. Chang, Y. G. Zhang, D. B. Harteneck, H. Choo, D. L. Olynick, S. Cabrini, *Nano Lett.* **2009**, *9*, 467.
- [22] G. M. Rutter, J. N. Crain, N. P. Guisinger, T. Li, P. N. First, J. A. Stroscio, *Science* **2007**, *317*, 219.
- [23] A. Reina, X. T. Jia, J. Ho, D. Nezich, H. B. Son, V. Bulovic, M. S. Dresselhaus, J. Kong, *Nano Lett.* **2009**, *9*, 30.